Wide Range Color Tuning in Single Emissive Layer Organic Light Emitting Transistors

Alexandre Bachelet, Sophie Fasquel, Jean-Michel Rampnoux, Gediminas Jonusauskas, Kazuo Takimiya, Lionel Hirsch, Mathias Perrin, Mamatimin Abbas

Wide Range Color Tuning in Single Emissive Layer Organic Light Emitting Transistors

Alexandre Bachelet [a], Sophie Fasquel [a], Jean-Michel Rampnoux [b], Gediminas Jonusauskas [b], Kazuo Takimiya [c,d], Lionel Hirsch [a], Mathias Perrin [b]* and Mamatimin Abbas [a]*

[a] Univ. Bordeaux, IMS, CNRS, UMR 5218, Bordeaux INP, ENSCBP, F-33405 Talence, France
[b] Univ. Bordeaux, LOMA, CNRS, UMR 5798, F-33405 Talence, France
[c] Emergent Molecular Function Research Team, RIKEN Center for Emergent Matter Science (CEMS), 2-1 Hirosawa, Wako, Japan
[d] Department of Chemistry, Graduate School of Science, Tohoku University, 6-3 Aoba, Aramaki, Aoba-Ku, Sendai, Japan

Abstract: Using a single emissive layer, color tuning within a wide visible light range (from blue to red) is achieved in organic light emitting transistors. In the fabricated devices, both the gate and drain electrodes are made of Aluminum (acting as an optical resonator), and the emissive layer thickness is adjusted to vary the distance between them. Remarkably, layer thickness variation which is responsible for color tuning do not affect the optical turn-on voltages, in contrast to organic light emitting diode devices. Significantly enhanced external quantum effeciencies are also observed for thick emissive layer devices. Optical simulations that accurately match experimental results indicate that the wide range of color tunability is mainly due to an outcoupling effect through the Fabry-Perot cavity. Our study presents a simpler and more flexible alternative for display technology design.

Keywords: organic semiconductors, light emitting transistors, optical resonator, color tuning

I. Introuduction

In the past 20 years, significant attention has been given to the study of organic semiconductors and their applications in electronics. The reason for this increased focus is due to their favorable properties in terms

of synthesis and processing, such as their ability to be easily tuned through chemical engineering and processed at room temperature on flexible substrates.[1] The research on organic light sources first focused on organic light-emitting diodes (OLED), then more recently, on organic light-emitting transistors (OLETs), which combine the current-switching and the light-emitting functions in a single device.[2,3] This double functionality has the potential to simplify circuit engineering in display applications, and OLETs are also being considered as a potential candidate for electrically pumped organic lasers due to their ability to sustain much higher current density compared to OLEDs.[4]

Over the past several years, there have been significant advancements in the development of OLETs. These advancements have led to improved device performance, and several architectures have been developed.[5–8] The use of asymmetric contacts for selectively injecting opposite charge carriers[4,9] and the use of separate transport and emissive layers[10,11] are among the key steps in this development. The challenge has been to find an organic molecule with both high mobility and high luminescence.[12] In multi-layered OLETs, the charge transport and light-emitting layers each offer their respective properties. A variety of high mobility charge transport layers have been applied, including small molecules, polymers, and metal oxides.[13–16] Many OLETs reported so far work at relatively high operating voltages ($\geq$ 60 V), which limits their practical use. To reduce the operating voltage, high-k dielectrics with polymer insulators or metal oxides have been explored.[7,17] Charge blocking/injection layers which are essential components in OLEDs can manifest their role in low-operating voltage OLETs.[18] Contrary to OLETs, efficiency enhancement and color tuning in microcavity OLEDs are well-established. For instance, the integration of a quarter wave dielectric stack (QWS) into OLEDs as a Bragg mirror was shown to improve the electroluminescence (EL) efficiency and resulted in a spectral variation of the EL with the viewing angle.[19] By patterning an optical filler on top of the QWS, the emission wavelength could be controlled over a range of 150 nm in Alq-based OLEDs. [20] Additionally, the electroluminescent spectra in Alq_3/TPD bi-layer OLEDs can vary significantly with the thickness of the light-emitting layer due to interference

effects.[21] Aluminum was used as both the cathode and anode in OLEDs (in a rare example) and resulted in an angle-dependent EL spectra for separate blue, green, and red emissive layer devices.[22] Microcavity OLEDs with Al semitransparent electrode also offered color tuning with the thickness variation, but with high optical turn-on voltages for thick samples.[23] In the present work, we demonstrate that OLET electroluminescent spectrum can be tuned over a wide visible light range, from blue to red, over 300 nm, by merely varying the thickness of the emissive layer. Low turn-on voltages are preserved even for thick samples and a high external quantum efficiency (EQE) can be achieved thanks to a modal engineering that improves the outcoupling efficiency and reduces losses.

II. Methods

The glass substrates (15mm x 15mm) were cleaned using Hellmanex soap in ultrapure water for 15 minutes in an ultrasonic bath, followed by rinsing twice in pure water for 5 minutes each. They were then subjected to a 10-minute UV-O_3 treatment. A 100nm thick aluminum layer was deposited as the gate using an e-beam deposition system with a base pressure of 1×10^{-6} mbar. The aluminum was partially anodized in a citric acid solution (0.1 mM) to obtain a 35nm thick Al_2O_3 as described earlier.[30] A thin layer of polystyrene (3mg/mL in chlorobenzene) was spin-coated (2000 rpm, 60s) to passivate the surface.[31] The transport layer, C_{10}-DNTT (20nm), was evaporated in a thermal evaporator at the base pressure of 1×10^{-6} mbar with a controlled rate of 0.1 to 0.2 Å s^{-1}. MoO_3 (10nm)/Ag (40nm) source electrode was deposited through a shadow mask with a rate of 0.1 nm s^{-1}. The emissive layer, Alq_3, was thermally evaporated at a rate of 0.5 Å s^{-1} with final thicknesses of 50 nm, 75 nm, 125 nm, 150 nm and 175 nm. The BCP hole blocking layer (10 nm) was deposited via organic evaporation deposition process, at a rate of 0.5 Å s^{-1}. Finally, the semitransparent drain electrode (LiF (1nm)/Al (15nm)) was deposited through a shadow mask. The channel length was 300 µm and channel width was 2 mm.

The characterizations were carried out under inert atmosphere (nitrogen glovebox). A 4200 Keithley Semi-conductor analyzer along with a calibrated silicon photodetector were used to measure the electrical and optical signals. A Hamamatsu amplifier was used to magnify the photocurrent. An optical fiber and

the Ocean Optics software were used to measure the EL spectra of the working devices. EL intensities were calculated taking into account the photo response of the Si detector and the EL spectrum of each device. EL spectra were normalized to give weight to each wavelength with respect to the contribution to the light output power. Thus, the number of photons in each wavelength was derived to obtain the total number of photons of each device at certain gate voltage. EQE was then calculated through the number of electrons determined by the current density. It is to be noted that although the area of the photodetector is much large than the emission area and as close as possible to the surface of the device, the light emitted from the sides was not collected. Therefore, the EQEs here are underestimated. An excitation wavelength of 380 nm was used to record PL spectrum. The photographs were taken using a Nikon D-80 camera with a 50 mm lens.

Numerical simulations were conducted in 3D to produce the reported results, and also in 2D, to test the models. We used home made programs based on Fourier Transformation of Maxwell equations in planar structures[32], as well as a transfer matrix[33] approach that generalizes to 3D exciton distributions. Both were compared to Comsol Multiphysics Finite Element Solver.

III. Results and discussion

In Figure 1, we present the device architecture of our OLET. The device consists of two active layers: 2,9-didecyl dinaphtho[2,3-b: 2', 3'-f] thieno[3,2-b] thiophene (C_{10}-DNTT) as the charge transport layer and Tris-(8-hydroxyquinoline)aluminum (Alq_3) as the emissive layer. Non-planar asymmetric contacts were applied, with molybdenum oxide (MoO_3)/Ag as the source electrode and lithium fluoride (LiF)/Al as the drain electrode. A hole blocking layer of Bathocuproine (BCP) was added following our previous study, which showed that blocking holes and efficiently injecting electrons can significantly enhance the optical performance of OLETs operating at low voltage.[18] A 35 nm of anodized Al_2O_3 passivated by polystyrene is proven to be an excellent dielectric bilayer with high capacitance (95 nF cm^{-2}), low interface traps and low leakage current, enabling the devices to operate at as low as 5 V.

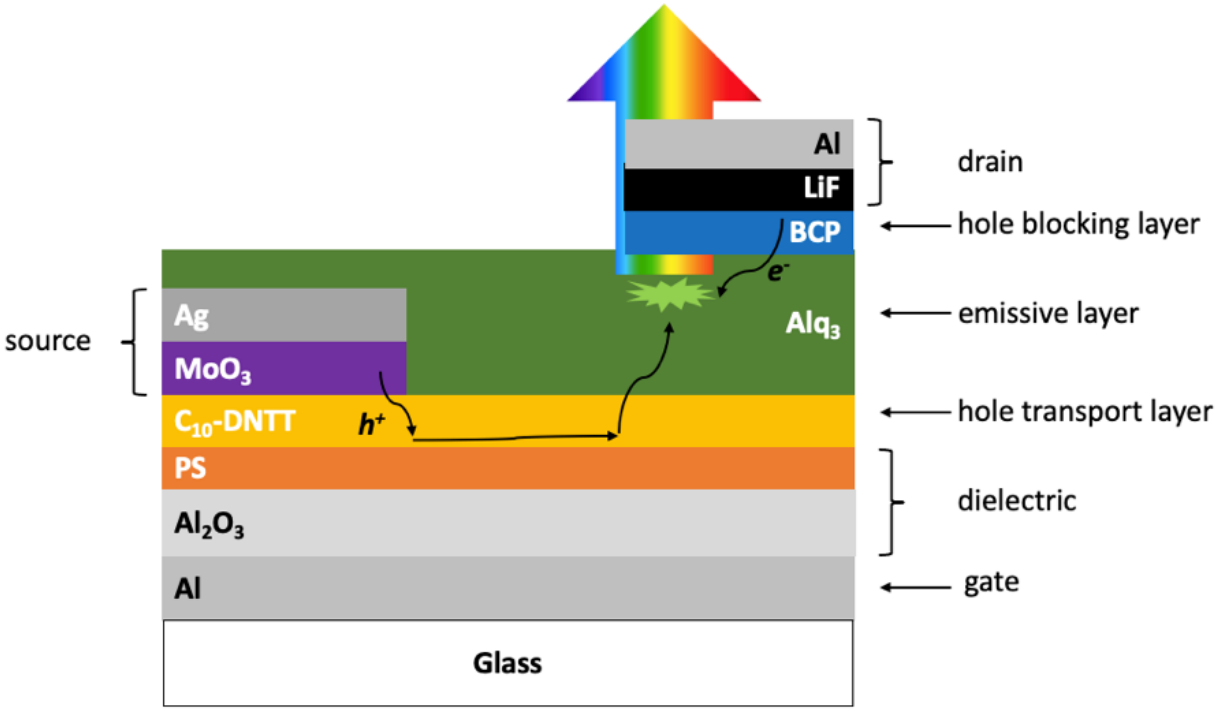

Figure 1 Device structure of the OLET (PS: polystyrene). MoO_3/Ag contact is grounded (source) for hole injection and fixed negative V_{ds} is applied to the LiF/Al contact (drain) for electron injection, which also allows light outcoupling as a semitransparent electrode.

In Figure 2 a), we present the typical transfer characteristics of the OLETs with varying thicknesses of the emissive layer (from 50 nm to 175 nm). Although they are overall similar, a slight dependence on the emissive layer thickness can be observed: the current maximum decreases as the layer thickness increases. Here the hole current is due to the positive charge injection from MoO_3/Ag contact into C_{10}-DNTT layer, followed by further transport to the drain electrode through Alq_3 emissive layer. This trend can be explained by the fact that low carrier mobility in Alq_3 affects slighly the transport when the thickness increases, consequently resulting in a lower current.[24] We have to emphasize though, in our device architecture of OLET, by applying negative gate and drain voltages, we injected, transported (through hole transport molecule) and extracted positive charges. What we have is the hole current in the circuit, meaning available abundant positive charges for recombination once the electrons are injected through the drain contact. Output characteristics (50 nm thick Alq_3) and all device performance parameters are given in the Supporting Information (Figure S1 and Table S1).

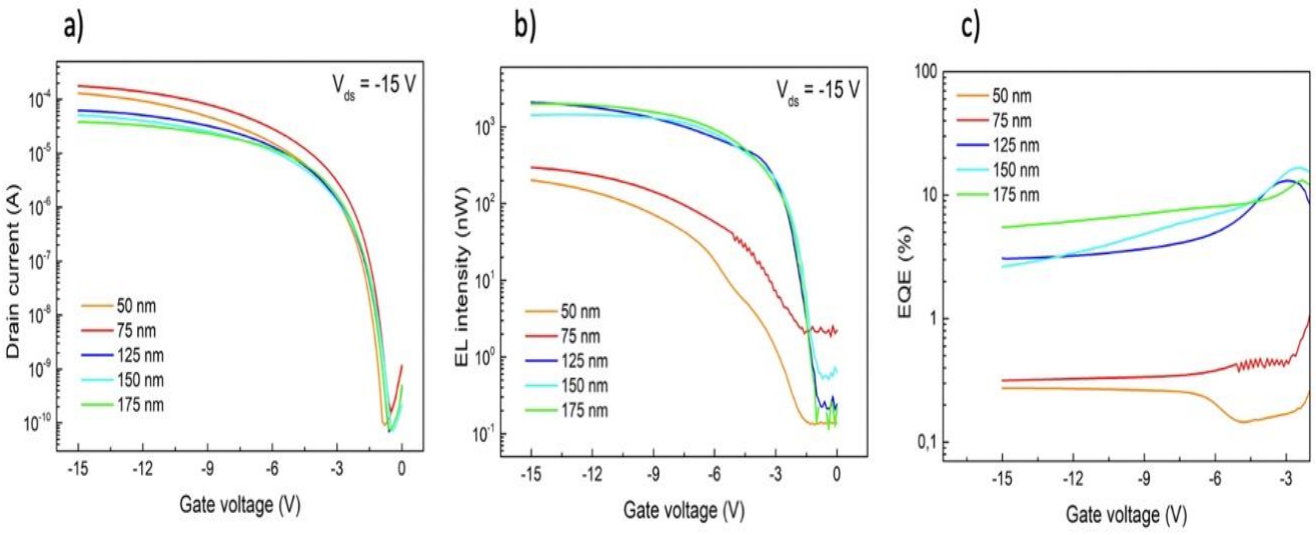

Figure 2 a) Typical transfer characteristics (V_{ds} = -15 V) of the OLET devices with the variation of the emissive layer thickness from 50 nm to 175 nm. b) Electroluminescence as a function of gate voltage for corresponding devices. c) External quantum efficiencies

Electroluminescence (EL) of OLETs as a function of the gate voltage is presented in Figure 2 b). We observed a significant increase in EL intensity when the emissive layer is thicker than 125 nm. Besides, we noticed that the turn-on voltages remained almost the same for thick emissive layer devices (-1.3 V), being even slightly smaller than thin emissive layer ones (-1.5 V). This is in contrast to what is known in OLEDs, whose turn-on voltages could significantly increase for thick active layers devices.[21,23] The fundamental difference in device structures between OLETs and OLEDs is the reason behind the observed difference. In OLETs, the number of charges injected depends on the gate voltage and the capacitance of the dielectric. The hole transport channel layer (in our case) mainly governs the charge transport and current density, while the emissive layer thickness has only a slight impact. On the other hand, in OLEDs, both carriers are transported by the emissive layer before recombination. Thicker active layers significantly reduce available number of charges for recombination, leading to an increase in the turn-on voltage. External quantum efficiency (EQE) of the thick layer devices is almost ten times higher than that of the thin layer devices, as shown in Figure 2 c). Oveall enhancement of EQEs in thicker layer devices will be explained in the latter part of the paper mainly taking into account optical loss mechanism. High EQEs around the gate voltage of 3 V can be attributed to the low electrical losses primarily due to significanly lower current density in this region. When current density increases through applied higher

gate voltage, exciton/carrier quenching becomes a major electrical loss mechanim, consequently decreasing EQEs. We clearly observed a change in color from blue to red in the devices. To confirm this, we measured the EL spectra of the OLETs, which are presented in Figure 3 a).

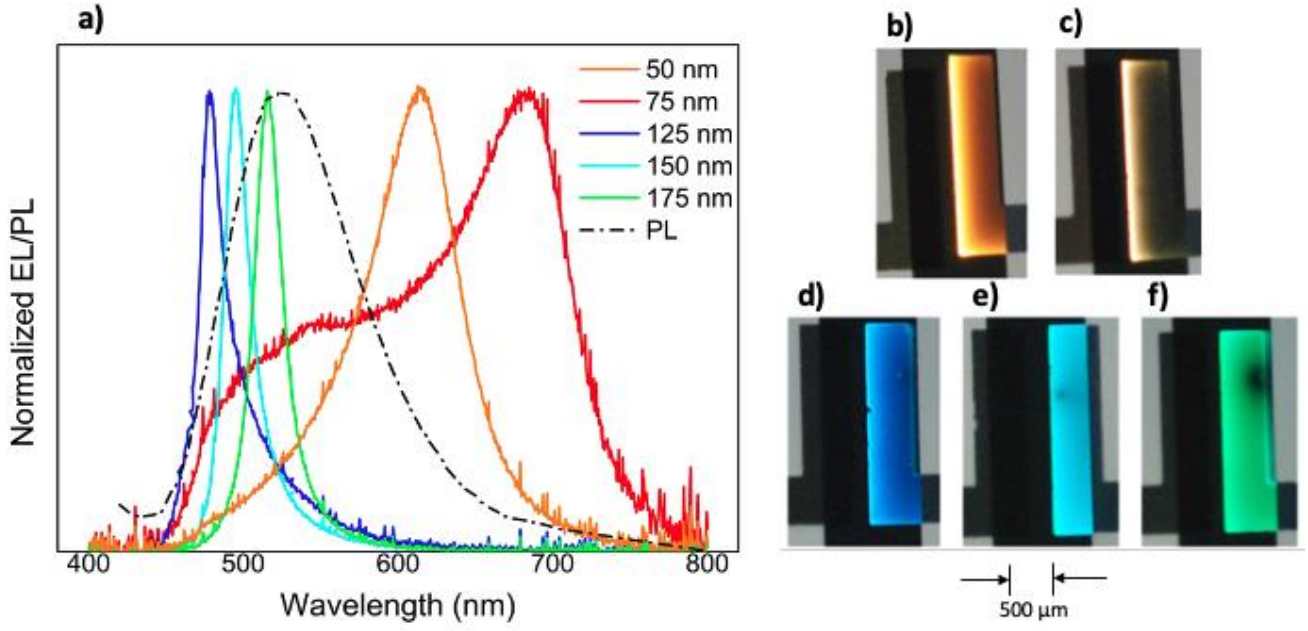

Figure 3 a) EL spectra (solid lines) of OLETs with different Alq_3 emissive layer thickness and PL spectrum (dashed dot line) of Alq_3 film; Microscopic photos of light emission from OLETs (at V_{ds}=-15 V, V_{gs}=-15 V) with Alq_3 thickness of b) 50 nm, c) 75 nm, d) 125 nm, e) 150 nm and f) 175 nm

PL of Alq_3 peaks at about 530 nm, emitting mainly green light. ELs of OLETs with Alq_3 thickness of 50 nm and 75 nm peak at about 620 nm and 690 nm, respectively, albeit still displaying minor emissions in the green region. When the Alq_3 emissive layer thickness exceeds 125 nm, the EL spectra become narrower and turns to blue. Futher increase in the layer thickness redshifts the peak. This color tuning is clearly evident in the microscopic images of the light emission from the OLETs, as demonstrated in Figures 3 b), c), d), e) and f) for the respective Alq_3 thicknesses.

In order to understand the EQE increase and spectrum dependancy of EL on Alq_3 thickness, we built an optical model of this Fabry-Pérot cavity with one exciton emitting inside. In principle, the spectral shape

of the light emitted by OLET depends on the Alq_3 PL spectrum and on two physical effects linked to the cavity architecture:

(i) The possible modification of the emission spectrum due to the coupling with a cavity resonance, that would *e.g.* enhance radiative transitions.[25]

(ii) The fact that light outcoupling, quantified by the power transmission through the drain electrode, denoted $T(\lambda)$, depends on the wavelength, because of the Fabry-Perot cavity and the dispersive properties of layers (particularly the electrodes).

Taking both effects into account, we computed the EL of emitted light and its power. We considered that optical transitions are enhanced by Purcell effect, whereas non-radiative transition remain unaffected.[26] This permits to derive a simple expression for the EL spectrum of light emitted by excitons inside the multilayer cavity, $I_{Em}(\lambda)$, versus the PL spectrum $I_{PL}(\lambda)$ and the Purcell factor $F(\lambda)$, that depends on the location and orientation of the exciton, taken as a point electric dipole source:

$$I_{Em}(\lambda) = \frac{I_{PL}(\lambda).F(\lambda)}{1-I_{PL}(\lambda)+I_{PL}(\lambda).F(\lambda)} \quad (1)$$

To compute the optical properties of the planar cavity, i.e. $F(\lambda)$, $T(\lambda)$, we took into account the leaky, evanescent and guided modes of the multilayer for TE and TM polarization. This technique (see Methods section), previously used for 3D dielectric cavity structures[27] allows us to achieve a quantitatively accurate representation of the spectral shape, as long as the layer thicknesses and refractive indices of the materials are known with precision. To compute the EL spectra, we considered a uniform tri-dimensional orientation of the exciton, and varied the exciton location in the vicinity (5 nm) of the emissive / hole blocking layer interface, as holes are much more mobile than electrons in Alq_3. Eventually, we calculated the radiated spectra, defined as: $I_{EL}(\lambda) = T(\lambda).I_{Em}(\lambda)$, and compared it to the experimental measurements. Note that the parameters we used for the numerical simulation were measured (layer thickness, refractive index) or taken from handbook. In particular, the refractive index of Aluminium was obtained by ellipsometry. This latter measurement was critical as Aluminium is known to be highly

reactive and its refractive index can vary significantly depending on the fabrication conditions.[28] The refractive index measured for drain and gate Aluminium are different, due to the different methods of deposition (see Supporting Information Figure S2). Our results show a good agreement between the model and the experiment, as shown in Figure 4. The minor discrepancies observed in the blue and green regions could be attributed to some inaccuracies in the refractive index at these wavelengths, or to slight departure from a uniform orientation of the excitons.

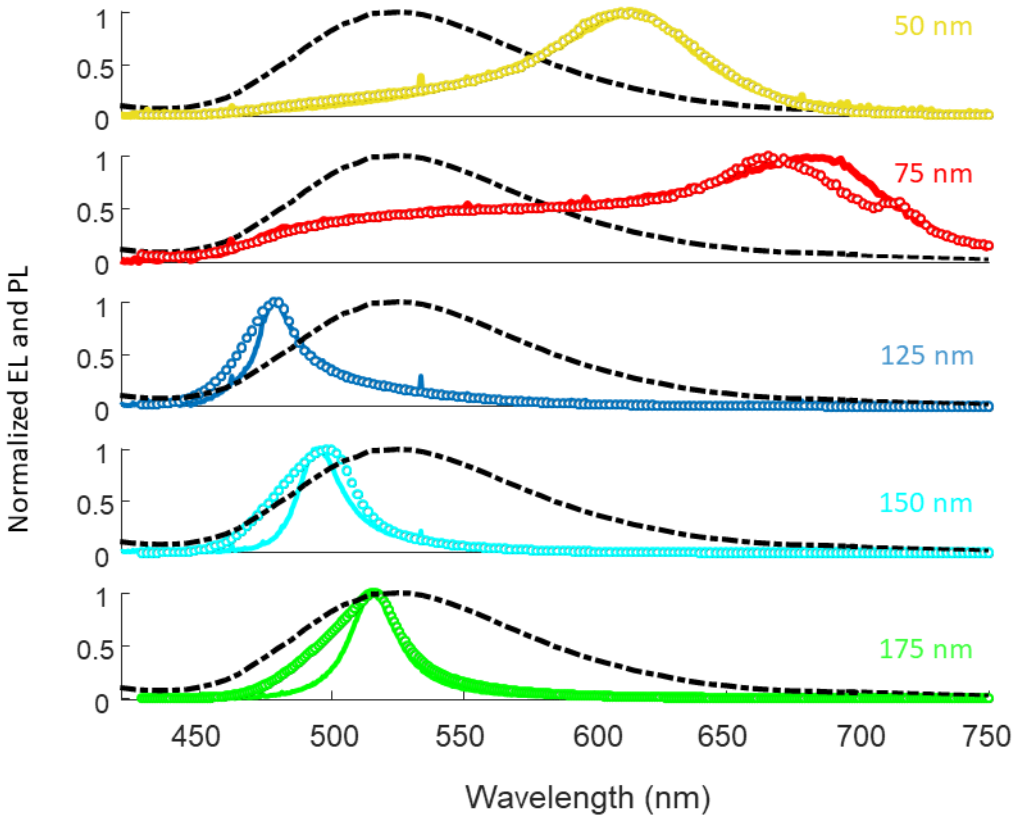

Figure 4 Comparison of the measured spectrum (solid line) and the spectrum modelled with Eq. (1) (symbols), for different thicknesses of Alq_3. Dashed black line is the PL, shown for reference. The computed EL intensity has been averaged on exciton orientation, and exciton location has been tuned (with a distance between 0 and 5 nm from the BCP / Alq_3 interface)

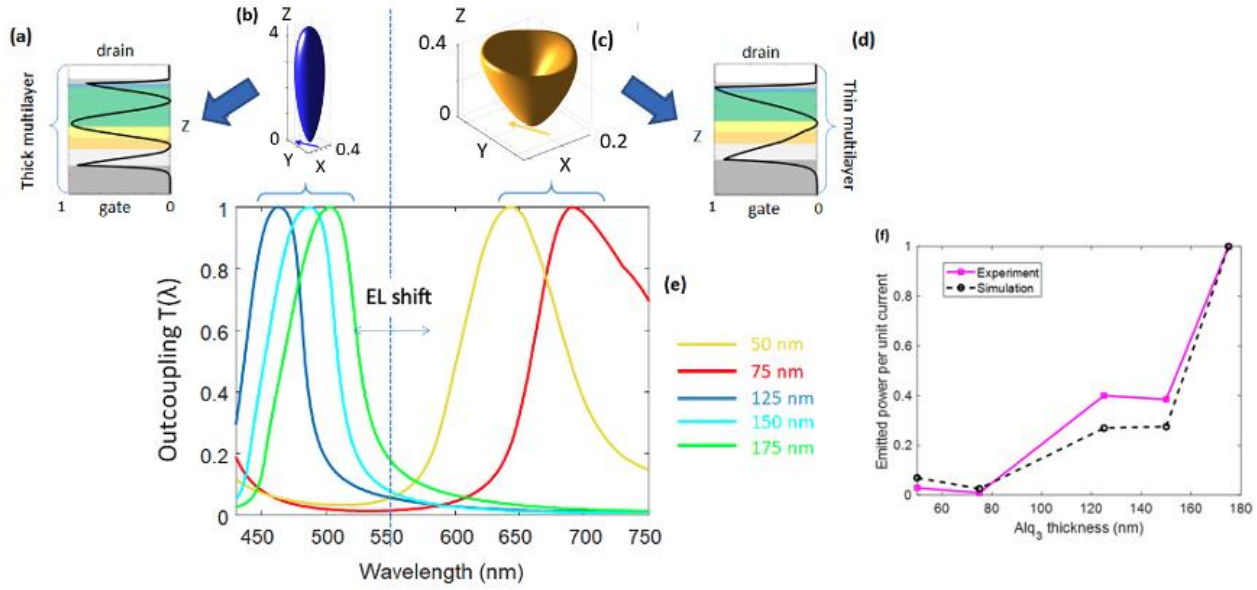

Figure 5 Optical properties of the OLET. Outcoupling through the drain (normalized to its maximum value), when an exciton located at the BCP / Alq_3 interface emits, for different thicknesses of Alq_3, panel (e). The near-field intensity profile of the leaky mode (represented along Z direction). The intensity profile of the leaky mode (along Z) is shown for 125 nm Alq_3 panel (a), and 50 nm Alq_3 panel (d). Colour code corresponds to the different OLET layers, see Figure 1. The far-field radiation diagram emitted by an exciton lying in XY plane is shown for 125 nm Alq_3 panel (b), and 50 nm Alq_3 panel (c). The power emitted in air for an exciton source is shown in panel (f), and compared to the experimental data obtained from Figure 3(a-b).

We then used numerical simulation to gain a better understanding of the effect. Figure 5 – see panel (e) – shows the outcoupling $T(\lambda)$ for different thicknesses of Alq_3. This value was calculated by integrating the transmission coefficients from the exciton point source through the drain and into the air for all plane waves, taking into account their intensities, directions, and polarizations, as shown in panels (b) and (c). By comparing Figure 5, panel (e) to Figure 3, we observed that the shape of T(λ) closely resembles the observed spectra. Furthermore, we found that the color tuning is primarily due to the wavelength-dependent transmission through the drain, and that the Purcell effect has only a minor impact on the emitted light spectrum in our configuration (see Supporting Information Figure S3).

Considering only the outcoupling effect, we are able to discuss the spectral changes of emitted light in a simpler manner. This light is carried away in the far-field, to the observer's eyes by leaky mode(s), whereas the energy stored in the guided mode(s) would remain inside, or in the vicinity of the multilayer

structure. Therefore, we focus on the properties of leaky modes for our architecture, see Figure S4. Figure 5, panels (a) and (d), display the intensity profile inside the multilayer of the leaky optical mode that is excited by the exciton recombination and carries energy out of the OLET towards the observer's eye. For all the thicknesses studied, only one leaky mode was present, but its characteristics changed with the total thickness of the multilayer. Its intensity profile inside the multilayer is shown Figure 5, panels (a) and (d), for two specific thicknesses (50nm and 125 nm). As expected, increasing Alq_3 layer thickness shifts its peak of excitation to longer wavelengths, see panel (e). For 50 nm and 75 nm Alq_3 layers, the first-order mode, which has one zero of intensity between the drain and gate, was excited (Figure 5(d)). For thicknesses above 75 nm, this mode shiftes out of the wavelength range where Alq_3 PL can excite it. The second-order mode, which has two zeros of intensity between the drain and gate (Figure 5(a)), can be excited by the short-wavelength side of Alq_3 PL (thicknesses between 125 nm to 175 nm). The energy of this latter mode is mainly contained within the lossless organic layers and interacts less strongly with the metallic layers. This leads to less losses[29] and higher quality factor for second order modes (125 nm to 175 nm Alq_3 layers), which have consequently much narrower spectra than first order modes (50 nm and 75 nm Alq_3 layers). The emitted power for an exiton source (a given current) is shown in Figure 5(f), and compared to the experiments. This confirms the substantial difference in EQE seen experimentally (refer to Figure 2 c)). Specifically, the dipole-like emission of thick layers (as shown in panel (b)) allows for more efficient extraction of light towards the observer, compared to the higher-order multipolar emission seen in thin layers (as seen in panel (c)).

A particular situation occurs for 75 nm, where the transmission peak is shifted far on the red side of PL, leading to a broad spectrum with a white reddish color, see Figure 3 a). Despite the rather small emitted intensity in such a case, as most of the light remains trapped in the guided modes, this example proves a remarkable fact: the EL spectral width can be increased, compared to PL width, just by adjusting the layer thickness.

IV. Conclusions

In summary, the study presents a device architecture in organic light-emitting transistors (OLETs) where both gate and drain electrodes are made of Aluminum, allowing for wide-range visible light color tuning with just a single Alq_3 emissive layer by changing its thickness. The results of optical simulations suggest that the spectral shift is mainly due to the wavelength-dependent outcoupling through the drain electrode, thus providing insight into the connection between the stack geometry and the location and width of the electroluminescence (EL) spectrum. The large increase in EQE for layers thicker than 100 nm comparing to thin layers (50 nm and 75 nm) is attributed to a change in the radiation diagram of the "exciton in cavity". This approach offers a flexible solution for color tuning in OLETs using a single emissive layer.

AUTHOR INFORMATION

Corresponding Authors
Mamatimin ABBAS : mamatimin.abbas@ims-bordeaux.fr
Mathias PERRIN : mathias.perrin@u-bordeaux.fr

Funding Sources

A. Bachelet acknowledges financial support of Bordeaux University Doctoral Grant. This work is also suppoted by Agence Nationale de la Recherche (IDOL, ANR-22-CE24-0010).

Notes

The authors declare no competing financial interests.

ASSOCIATED CONTENT

Supporting Information

Supporting Information Available: output characteristics curves; device performance parameters table; comparison of the refractive index of Al deposited thermally and with e-beam; effect of Purcell on emission spectrum; Modes of the OLET with 50nm Alq_3 layer. This material is available free of charge via the Internet at http://pubs.acs.org

References

(1) Forrest, S. R. The Path to Ubiquitous and Low-Cost Organic Electronic Appliances on Plastic. *Nature* **2004**, *428* (6986), 911–918. https://doi.org/10.1038/nature02498.
(2) Muccini, M. A Bright Future for Organic Field-Effect Transistors. *Nat. Mater.* **2006**, *5* (8), 605–613. https://doi.org/10.1038/nmat1699.
(3) Chaudhry, M. U.; Muhieddine, K.; Wawrzinek, R.; Sobus, J.; Tandy, K.; Lo, S. C.; Namdas, E. B. Organic Light-Emitting Transistors: Advances and Perspectives. *Adv. Funct. Mater.* **2020**, *30*

(20), 1–15. https://doi.org/10.1002/adfm.201905282.
(4) Takahashi, T.; Takenobu, T.; Takeya, J.; Iwasa, Y. Ambipolar Light-Emitting Transistors of a Tetracene Single Crystal. *Adv. Funct. Mater.* **2007**, *17* (10), 1623–1628. https://doi.org/10.1002/adfm.200700046.
(5) Hepp, A.; Heil, H.; Weise, W.; Ahles, M.; Schmechel, R.; von Seggern, H. Light-Emitting Field-Effect Transistor Based on a Tetracene Thin Film. *Phys. Rev. Lett.* **2003**, *91* (15), 157406. https://doi.org/10.1103/PhysRevLett.91.157406.
(6) Gwinner, M. C.; Kabra, D.; Roberts, M.; Brenner, T. J. K.; Wallikewitz, B. H.; McNeill, C. R.; Friend, R. H.; Sirringhaus, H. Highly Efficient Single-Layer Polymer Ambipolar Light-Emitting Field-Effect Transistors. *Adv. Mater.* **2012**, *24* (20), 2728–2734. https://doi.org/10.1002/adma.201104602.
(7) Soldano, C.; D'Alpaos, R.; Generali, G. Highly Efficient Red Organic Light-Emitting Transistors (OLETs) on High-k Dielectric. *ACS Photonics* **2017**, *4* (4), 800–805. https://doi.org/10.1021/acsphotonics.7b00201.
(8) Sobus, J.; Bencheikh, F.; Mamada, M.; Wawrzinek, R.; Ribierre, J. C.; Adachi, C.; Lo, S. C.; Namdas, E. B. High Performance P- and n-Type Light-Emitting Field-Effect Transistors Employing Thermally Activated Delayed Fluorescence. *Adv. Funct. Mater.* **2018**, *28*, 1800340. https://doi.org/10.1002/adfm.201800340.
(9) Nakamura, K.; Ichikawa, M.; Fushiki, R.; Kamikawa, T.; Inoue, M.; Koyama, T.; Taniguchi, Y. Light Emission from Organic Single-Crystal Field-Effect Transistors. *Jpn. J. Appl. Phys.* **2005**, *44* (No. 44), L1367--L1369. https://doi.org/10.1143/jjap.44.l1367.
(10) Namdas, E. B.; Ledochowitsch, P.; Yuen, J. D.; Moses, D.; Heeger, A. J. High Performance Light Emitting Transistors. *Appl. Phys. Lett.* **2008**, *92* (18), 2008–2010. https://doi.org/10.1063/1.2920436.
(11) Capelli, R.; Toffanin, S.; Generali, G.; Usta, H.; Facchetti, A.; Muccini, M. Organic Light-Emitting Transistors with an Efficiency That Outperforms the Equivalent Light-Emitting Diodes. *Nat. Mater.* **2010**, *9* (6), 496–503. https://doi.org/10.1038/nmat2751.
(12) Zaumseil, J.; Sirringhaus, H. Electron and Ambipolar Transport in Organic Field-Effect Transistors. *Chem. Rev.* **2007**, *107* (4), 1296–1323. https://doi.org/10.1021/cr0501543.
(13) Ullah, M.; Wawrzinek, R.; Nagiri, R. C. R.; Lo, S.; Namdas, E. B. UV–Deep Blue–Visible Light-Emitting Organic Field Effect Transistors with High Charge Carrier Mobilities. *Adv. Opt. Mater.* **2017**, *5*, 1600973.
(14) Ullah, M.; Armin, A.; Tandy, K.; Yambem, S. D.; Burn, P. L.; Meredith, P.; Namdas, E. B. Defining the Light Emitting Area for Displays in the Unipolar Regime of Highly Efficient Light Emitting Transistors. *Sci. Rep.* **2015**, *5*, 8818. https://doi.org/10.1038/srep08818.
(15) Muhieddine, K.; Ullah, M.; Pal, B. N.; Burn, P.; Namdas, E. B. All Solution-Processed, Hybrid Light Emitting Field-Effect Transistors. *Adv. Mater.* **2014**, *26* (37), 6410–6415. https://doi.org/10.1002/adma.201400938.
(16) Ablat, A.; Kyndiah, A.; Bachelet, A.; Takimiya, K.; Hirsch, L.; Fasquel, S.; Abbas, M. Low Optical Turn-on Voltage in Solution Processed Hybrid Light Emitting Transistor. *Appl. Phys. Lett.* **2019**, *115*, 023301. https://doi.org/10.1063/1.5090220.
(17) Chaudhry, M. U.; Tetzner, K.; Lin, Y. H.; Nam, S.; Pearson, C.; Groves, C.; Petty, M. C.; Anthopoulos, T. D.; Bradley, D. D. C. Low-Voltage Solution-Processed Hybrid Light-Emitting Transistors. *ACS Appl. Mater. Interfaces* **2018**, *10* (22), 18445–18449. https://doi.org/10.1021/acsami.8b06031.
(18) Bachelet, A.; Chabot, M.; Ablat, A.; Takimiya, K.; Hirsch, L.; Abbas, M. Low Voltage Operating Organic Light Emitting Transistors with Efficient Charge Blocking Layer. *Org. Electron.* **2021**, *88*, 106024. https://doi.org/10.1016/j.orgel.2020.106024.
(19) Jordan, R. H.; Rothberg, L. J.; Dodabalapur, A.; Slusher, R. E. Efficiency Enhancement of

Microcavity Organic Light Emitting Diodes. *Appl. Phys. Lett.* **1996**, *69* (14), 1997–1999. https://doi.org/10.1063/1.116858.
(20) Dodabalapur, A.; Rothberg, L. J.; Jordan, R. H.; Miller, T. M.; Slusher, R. E.; Phillips, J. M. Physics and Applications of Organic Microcavity Light Emitting Diodes. *J. Appl. Phys.* **1996**, *80* (12), 6954–6964. https://doi.org/10.1063/1.363768.
(21) So, S. K.; Choi, W. K.; Leung, L. M.; Neyts, K. Interference Effects in Bilayer Organic Light-Emitting Diodes. *Appl. Phys. Lett.* **1999**, *74* (14), 1939–1941. https://doi.org/10.1063/1.123734.
(22) Lee, C. J.; Park, Y. Il; Kwon, J. H.; Park, J. W. Microcavity Effect of Top-Emission Organic Light-Emitting Diodes Using Aluminum Cathode and Anode. *Bull. Korean Chem. Soc.* **2005**, *26* (9), 1344–1346. https://doi.org/10.5012/bkcs.2005.26.9.1344.
(23) Dahal, E.; Allemeier, D.; Isenhart, B.; Cianciulli, K.; White, M. S. Characterization of Higher Harmonic Modes in Fabry–Pérot Microcavity Organic Light Emitting Diodes. *Sci. Rep.* **2021**, *11*, 8456. https://doi.org/10.1038/s41598-021-87697-8.
(24) Fong, H. H.; So, S. K. Hole Transporting Properties of Tris(8-Hydroxyquinoline) Aluminum (Alq3). *J. Appl. Phys.* **2006**, *100* (9), 094502. https://doi.org/10.1063/1.2372388.
(25) Furno, M.; Meerheim, R.; Hofmann, S.; Lüssem, B.; Leo, K. Efficiency and Rate of Spontaneous Emission in Organic Electroluminescent Devices. *Phys. Rev. B - Condens. Matter Mater. Phys.* **2012**, *85* (11), 1–21. https://doi.org/10.1103/PhysRevB.85.115205.
(26) Chen, X.-W.; Choy, W. C. H.; He, S. Efficient and Rigorous Modeling of Light Emission in Planar Multilayer Organic Light-Emitting Diodes. *J. Disp. Technol.* **2007**, *3* (2), 110–117.
(27) Bertrand, A.; Dumur, F.; Mruczkiewicz, M.; Perrin, M.; Lartigau-Dagron, C.; Bousquet, A.; Vignau, L.; Billona, L.; Fasquel, S. Bottom-up Honeycomb Top Layer for Light Outcoupling Enhancement in Blue Organic Light Emitting Diodes. *Org. Electron.* **2017**, *52*, 222–229. https://doi.org/10.1016/j.orgel.2017.10.022.
(28) McPeak, K. M.; Jayanti, S. V.; Kress, S. J. P.; Meyer, S.; Iotti, S.; Rossinelli, A.; Norris, D. J. Plasmonic Films Can Easily Be Better: Rules and Recipes. *ACS Photonics* **2015**, *2* (3), 326–333. https://doi.org/10.1021/ph5004237.
(29) Lozan, O.; Perrin, M.; Ea-Kim, B.; Rampnoux, J. M.; Dilhaire, S.; Lalanne, P. Anomalous Light Absorption around Subwavelength Apertures in Metal Films. *Phys. Rev. Lett.* **2014**, *112* (19), 193903. https://doi.org/10.1103/PhysRevLett.112.193903.
(30) Abbas, M.; Cakmak, G.; Tekin, N.; Kara, A.; Guney, H. Y.; Arici, E.; Sariciftci, N. S. Water Soluble Poly(1-Vinyl-1,2,4-Triazole) as Novel Dielectric Layer for Organic Field Effect Transistors. *Organic Electronics*. 2011, pp 497–503. https://doi.org/10.1016/j.orgel.2010.12.023.
(31) Houin, G.; Duez, F.; Garcia, L.; Cantatore, E.; Hirsch, L.; Belot, D.; Pellet, C.; Abbas, M. Device Engineering for High Performance, Low Voltage Operating Organic Field Effect Transistor on Plastic Substrate. *Flex. Print. Electron.* **2017**, *2* (4), 45004. https://doi.org/10.1088/1361-665X/aa8886.
(32) Perrin, M.; Gruy, F. Explicit Calculation of Singular Integrals of Tensorial Polyadic Kernels. *Q. Appl. Math.* **2022**, *81* (1), 65–86. https://doi.org/10.1090/qam/1629.
(33) Benisty, H.; Stanley, R.; Mayer, M. Method of Source Terms for Dipole Emission Modification in Modes of Arbitrary Planar Structures. *J. Opt. Soc. Am. A* **1998**, *15* (5), 1192–1201. https://doi.org/10.1364/JOSAA.15.001192.

For Table of Contents Use Only

Alexandre Bachelet, Sophie Fasquel, Jean-Michel Rampnoux, Gediminas Jonusauskas, Kazuo Takimiya, Lionel Hirsch, Mathias Perrin* and Mamatimin Abbas*

Wide Range Color Tuning in Single Emissive Layer Organic Light Emitting Transistors

From blue to red color tuning is achieved using a single Alq_3 emissive layer in organic light emitting transistors in which Al gate and drain contacts form a cavity structure. Light enhancement and spectral narrowing are observed due to this cavity effect.

TOC Graphic